



## Research Article



# Modeling and survival exploration of breast carcinoma: A statistical, maximum likelihood estimation, and artificial neural network perspective

Anum Shafiq<sup>a,b,\*</sup>, Andaç Batur Çolak<sup>c</sup>, Tabassum Naz Sindhu<sup>d,\*\*</sup>, Showkat Ahmad Lone<sup>e</sup>, Tahani A. Abushal<sup>f,\*\*</sup>

<sup>a</sup> School of Mathematics and Statistics, Nanjing University of Information Science and Technology, Nanjing 210044, China

<sup>b</sup> Jiangsu International Joint Laboratory on System Modeling and Data Analysis, Nanjing University of Information Science and Technology, Nanjing 210044, China

<sup>c</sup> Information Technologies Application and Research Center, İstanbul Commerce University, İstanbul 34445, Türkiye

<sup>d</sup> Department of Statistics, Quaid-i-Azam University 45320, Islamabad 44000, Pakistan

<sup>e</sup> Department of Basic Sciences, College of Science and Theoretical Studies, Saudi Electronic University, Jeddah-M, Riyadh 11673, Kingdom of Saudi Arabia

<sup>f</sup> Department of Mathematical Science, Faculty of Applied Science, Umm Al-Qura University, Makkah, Saudi Arabia

## ARTICLE INFO

## ABSTRACT

**Keywords:**

Risk Function  
Reliability function  
Multi-layer perceptrons  
Artificial neural network  
Maximum likelihood estimation

The core objective of this research is to describe the behavior of the distribution using the MLE method to estimate its parameters, as well as to determine the optimal Artificial Neural Network method by comparing it to the maximum likelihood estimation method and applying it to real data for breast cancer patients to determine survival, risk, and other survival study functions of the log-logistic distribution. The parameters were defined in the input layer of the artificial neural network developed for the purpose of survival analysis and reliability function, hazard rate function, probability density function, reserved hazard rate function, Mills ratio, Odd function and CHR values were obtained in the output layer. The findings show that risk function increases with the increase in the time of infection and then decreases for a group of breast cancer patients under study, which corresponds to the theoretical properties of this according to the practical conclusions. The examination of survival analysis reveals that practical conclusions correspond to the theoretical properties of log-logistic distribution. Artificial neural networks have proven to be one of the ideal tools that can be used to predict various vital parameters, especially survival of cancer patients, with their high predictive capabilities.

## 1. Introduction

Any carcinoma that develops in our bodies is inherently harmful. If it occurs, we must endeavor to detect it and expel it as soon as possible. Breast carcinoma is an extremely frequent carcinoma in women of all races and ethnicities, and it is the second leading root of carcinoma-related death in Asian Pacific Islander, American-Indian Native women [1,2]. It is a carcinoma that begins in the tissues of the breast and spreads uncontrollably to other regions of the body, resulting in death. There are some occurrences of breast carcinoma in men, although they account for less than 0.05 percent of all occurrences symptomatic [3]. Breast carcinoma is grouped into two categories. The ducts that carry milk from the breast to the nipple are where ductal carcinoma begins. This is the most frequent types of breast carcinoma. Lobular cancer develops in the milk-producing lobules of the breast [4–6]. Bust

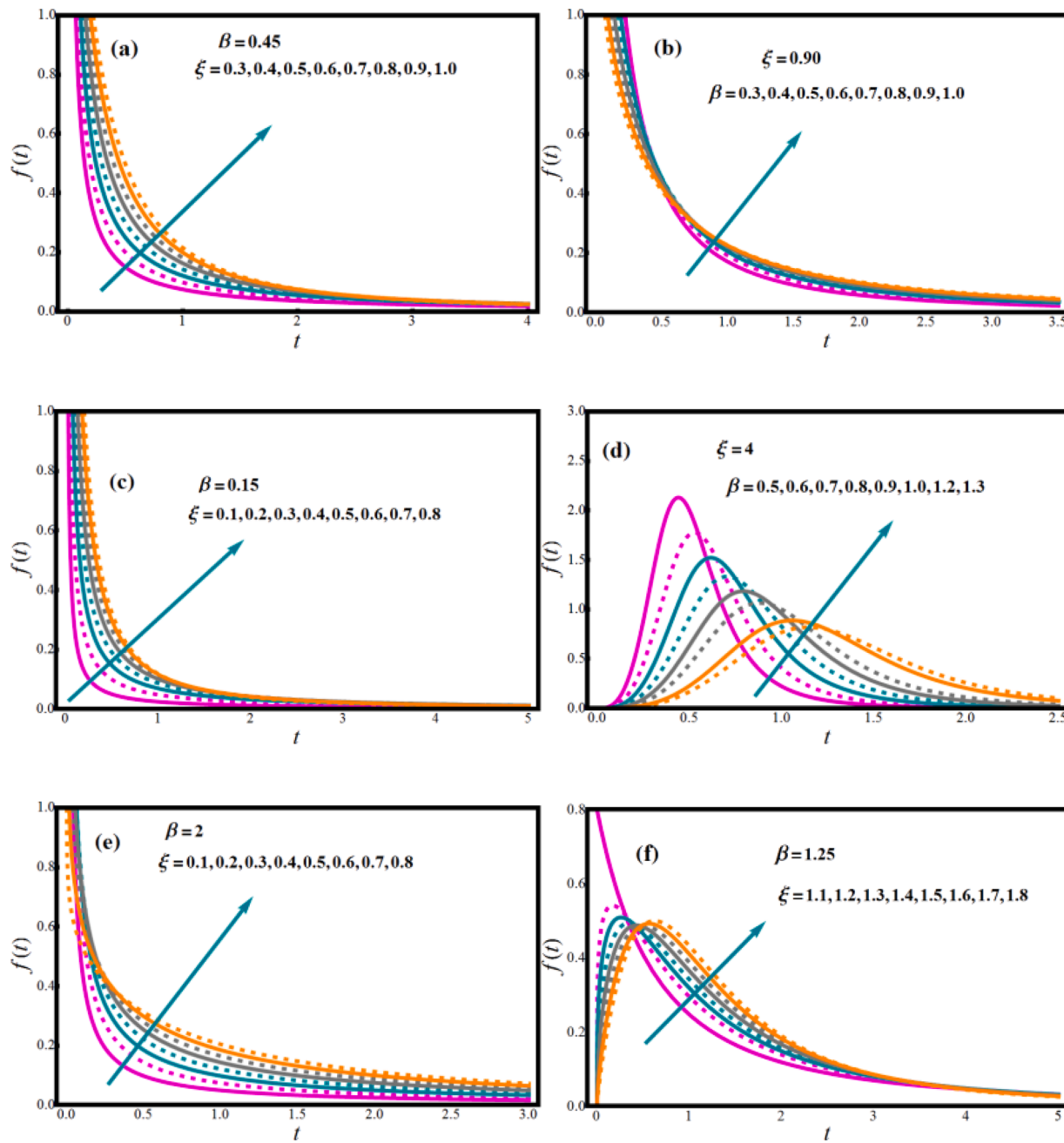
carcinoma can start in other parts of the breast in extremely uncommon circumstances. The three most significant things we can perform to discover a potentially malignant deepen in the breast are frequent mammography, annual clinical breast checks with your health practitioner, and monthly bust inspections [7].

Artificial intelligence tools, including artificial neural networks (ANN), have been used frequently in the projection of many health data, including oncological conditions [8–10]. There are some publications on the practice of ANNs that can predict data according to traditional statistical methods and mathematical tools. Ambrogi et al. [11] focused on the research of precise hazard functions of survival data as a statistical analysis. In the study, a multilayer perceptron is recommended as an addition of GLMs (generalized linear models) with multinomial errors using a nonlinear estimator within the structure of discrete-time distributions and competing risks. As per standard practice, weight reduction

\* Corresponding author at: School of Mathematics and Statistics, Nanjing University of Information Science and Technology, Nanjing 210044, China

\*\* Corresponding author.

E-mail addresses: [anumshafiq@ymail.com](mailto:anumshafiq@ymail.com) (A. Shafiq), [sindhuqau@gmail.com](mailto:sindhuqau@gmail.com) (T.N. Sindhu), [taabushal@uqu.edu.sa](mailto:taabushal@uqu.edu.sa) (T.A. Abushal).

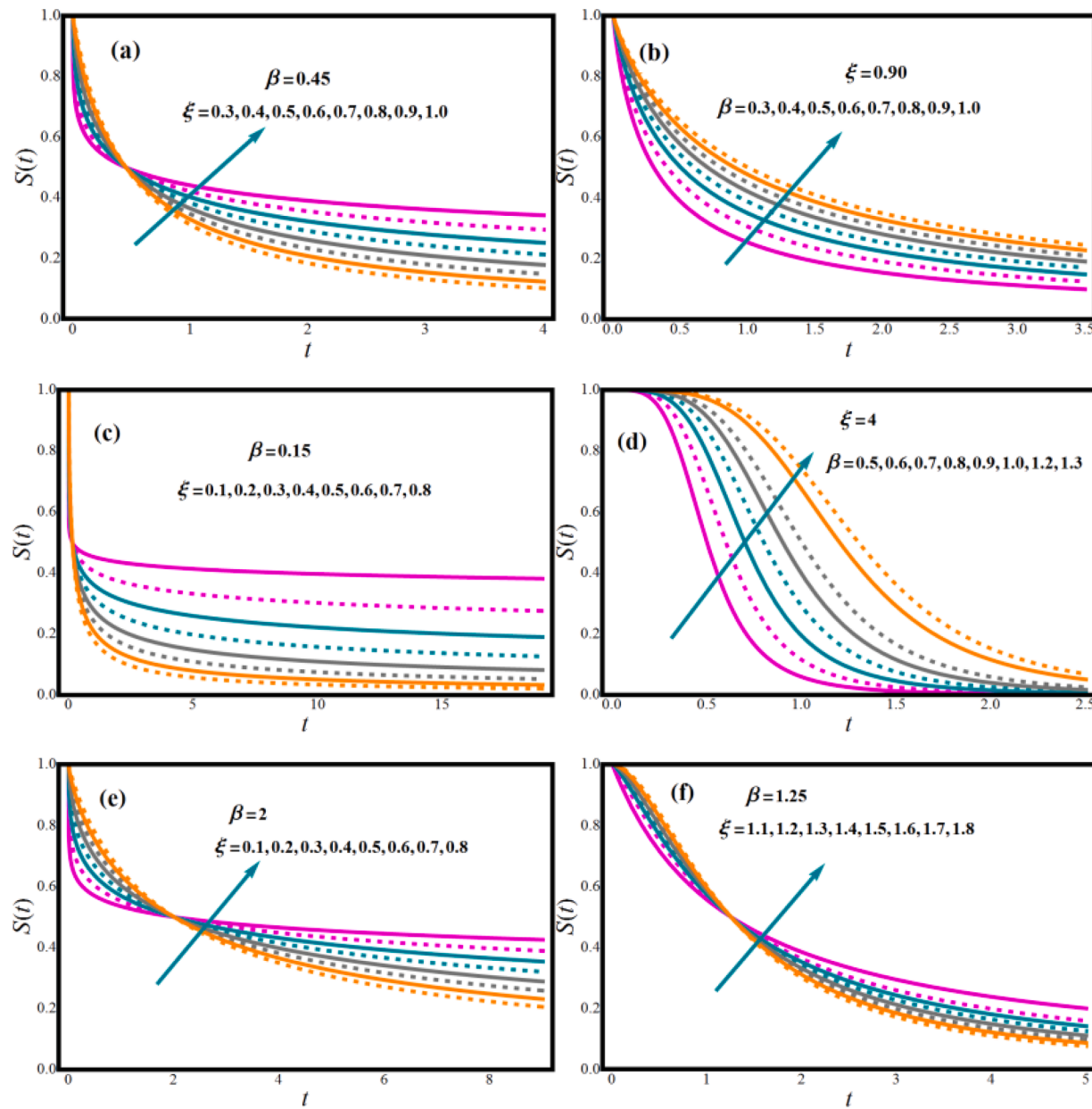


**Fig. 1.** Features of  $\xi$  and  $\beta$  on PDF of LL distribution

is adopted to modulate model complexity. For complexity control, a Genetic Algorithm is taken into account that allows each parameter of the model to be regulated independently. To exemplify the importance and strengths of the methodology, an implementation is presented on analyses of 1793 women with primary breast cancer without axillary lymph node involvement. Shafiq et al. [12] used two separate techniques, ANN modelling and maximum likelihood estimation (MLE), to establish a real application to estimate COVID-19 mortality rates in Italy. The numerical findings were compared to the predictions derived from the ANN model formed with 9 neurons in the hidden layer. The R value for ANN model was 0.99836, and the greatest deviance was -0.14%. The findings of the investigation showed the great reliability of the two statistical models constructed. Bhambhani et al. [13] examined the predictability of survival with machine learning in bladder cancer patients. In the research, the performance of ANN, a kind of machine learning algorithm, was evaluated with the performance of multivariate

Cox proportional hazards models in predicting 5-year genetic disorder survival and overall longevity. ANNs were trained and tested by dividing the dataset in a ratio of 80/20. Considering the inherent constraints of administrative datasets, machine learning can help to analyze the complex data they contain more effectively. As a result, it has been seen that machine learning algorithms can be a tool that can be used in improving the capacity to forecast the prognosis of breast carcinoma.

The log-logistic (LL) distribution is a significant right-skewed model that has piqued the researchers' interest [14]. It is employed as a survival study parametric model. The LL distribution, unlike the more often employed Weibull model, can have a non-monotonic hazard function for  $\xi > 1$ , where  $\xi$  is the shape indicator. Furthermore, for  $\xi \leq 1$ , the LL distribution's hazard function is unimodal and monotonically declining [15,16]. Some other feature of the LL distribution is that the model's function may be stated in explicit form, which is helpful in censored survival analysis. Further literature on the LL distribution's applications

Fig. 2. Features of  $\xi$  and  $\beta$  on SF

can be found in [17,18]. The LL distribution has been investigated by many scientists. The order statistics of the LL distribution were studied by [14]. Ali and Khan [19] developed recurrence equations for the LL distributions' moments of order statistics.

Because of its widespread application in biosciences and pharmacological studies, research in the domain of survival analysis has exploded in recent years. One goal of this research is to investigate the effectiveness of competing survival function estimators after selecting the probability density function (PDF) that perfectly describes the survival times of breast carcinoma women. The current study will employ the LL distribution to model survival data. Based on our careful review of abovementioned studies, we believe that no investigation has been conducted on metric analysis of the probability survival model via MLE and artificial ANN. Hence, the fundamental goal of this research is to investigate, optimize and predict lifetime model dependability using two different methodologies, ANN modelling and MLE. This research attempts to fill a significant gap in the existing literature.

We devoted a lot of time and exertion into this investigation in order

to make a fair comparison by integrating two techniques to model survival/failure times for breast cancer patients entry to the center until discharge was recorded, and that all of them were in a state of death upon discharge at Medical City Hospital - Baghdad for the year 2020 using LL distribution and enhancing it utilizing ANN modeling and MLE likewise.

This study is planned in accordance with current trends.

- The main goal of this research is to forecast and assess the dependability characteristics of LL distribution employing a set of inputs in all ANN models that has never been studied and addressed previously.
- To develop ANN-based models for forecasting the LL distribution's appealing closed-form features.
- Determine whether ANN models are ideal for assessing and forecasting features of real-world facts using the LL distribution.
- To assess results using two techniques.

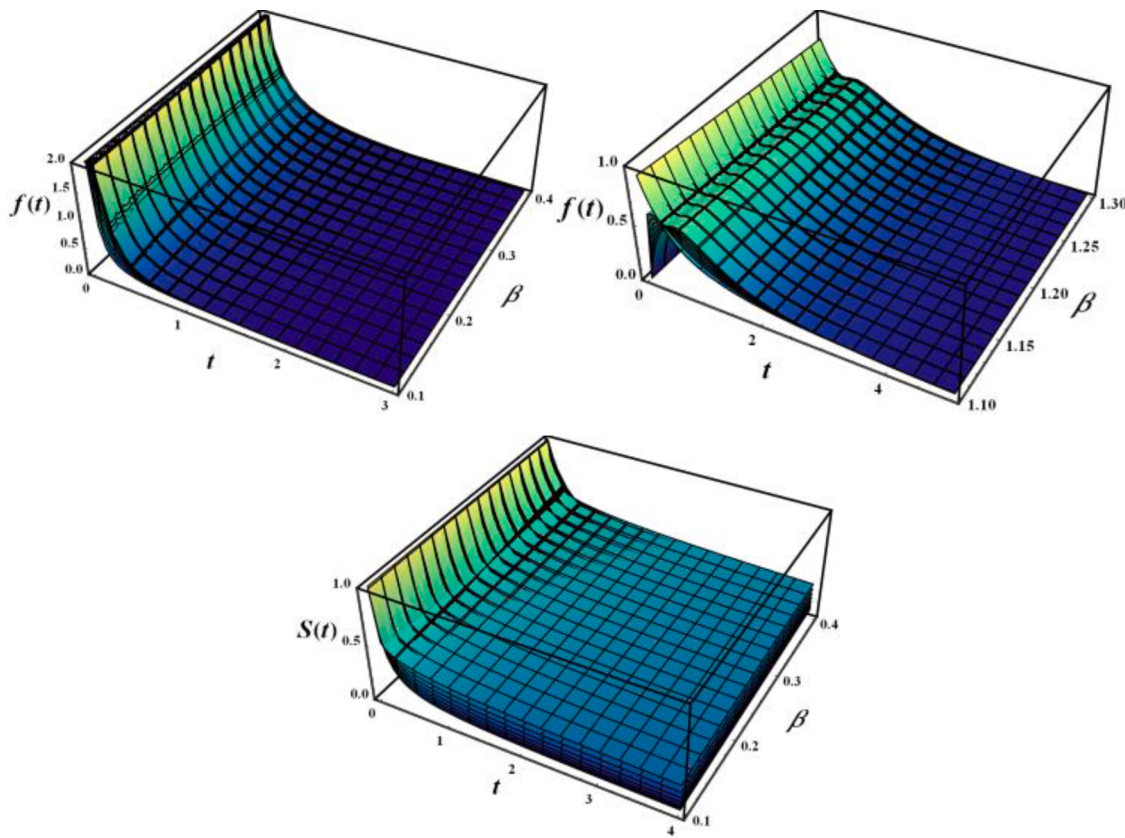


**Fig. 3.** 3D profiles of PDF and SF with rising  $\xi$ .

## 2. LL model and survival metrics

The CDF (cumulative distribution function) of  $r.v$  (random variable)  $T$  represents the probability that survival time is less than some value  $t$  with shape parameter  $\xi$  and scale parameter  $\beta$  is given by

$$\bar{G}(t|\xi, \beta) = \left\{ 1 + \left( \frac{t}{\beta} \right)^{-\xi} \right\}^{-1}, t, \xi, \beta > 0, \quad (1)$$

and PDF of LL distribution is

$$f(t|\xi, \beta) = \frac{\left( \frac{\xi}{\beta} \right) \left( \frac{t}{\beta} \right)^{\xi-1}}{\left\{ 1 + \left( \frac{t}{\beta} \right)^{\xi} \right\}^2}, t, \xi, \beta > 0. \quad (2)$$

Because of its flexibility and ability to imitate skewed data as shown in Fig. 1(a-f), the LL distribution is frequently employed in disciplines such as biological studies, dependability, physical infrastructure, and survival analysis.

In fields like as medicine biology, social sciences, econometrics, and engineering, survival analysis is now widely used [20]. Whenever it concerns to events that can happen over a long period of time (years), the time of occurrence becomes critical information, and the field that investigates its model is known as survival evaluation [17,21]. The period between a certain starting point (birth, commencement of treatment) and a "terminal" event (death, treatment failure), where "terminal" denotes that following events are not taken into account even if they could theoretically occur (i.e., recurrent failures), is referred to as survival time ( $T$ ). The survival function (SF) is the fundamental quantity for defining survival time  $T$  (nonnegative continuous  $r.v$ ) in this scenario. It is described as the likelihood of surviving at  $t$ :  $S(t) = \Pr(T > t) = 1 - \bar{G}(t)$ , as a result, the probabilities in the right tail of the distribution are given. Where, lifespan  $r.v T$  represents an individual's longevity. The

SF  $S(t|\xi, \beta)$  of LL distribution is.

$$S(t|\xi, \beta) = \left\{ 1 + \left( \frac{t}{\beta} \right)^{\xi} \right\}^{-1}, t, \xi, \beta > 0. \quad (3)$$

It's a monotonic decreasing function that assumes value one for  $t=0$  and ends at 0 as time approaches infinity. Fig. 2 illustrates graphs of the LL distribution's survival function for various parameter values. Under the considered parametric parameters, this displays monotonic non-increasing behavior. In Fig. 3, the 3D behavior of both  $f(t)$  and  $S(t)$  functions is shown.

The hazard rate is a measurement of an item's inclination to fail or perish based on its age. It is a subcategory of the larger field of statistics known as survival analysis. It's utilized to model a person's odds of dying as a function of age, and it's also utilized to model the periods with the largest and smallest possibilities of an occurrence. It can also be used to simulate any other variable that changes over time [22]. Let  $T$   $r.v$  represents the survival time, which is nothing but the time-to-event, then generally  $h(t)$ , is mathematically characterized as:

$$h(t) = \lim_{\Delta t \rightarrow 0^+} \frac{1}{\Delta t} P[t \leq T < t + \Delta t | T \geq t] \quad (4)$$

The hazard rate can be linked to its failure rate that is  $h(t) = -S'_T(t)/S_T(t)$ . The results from (3) to (4) demonstrate that the hazard rate and survival functions provide alternative but related descriptions of the  $T$  distribution. These are some of the reasons why using the hazard rate function instead of other techniques for presenting survival studies might be a beneficial suggestion:

- It is informative to evaluate the risk associated with an entity that is surviving at age  $t$ .
- effective for comparing groups of individuals,
- When there is censoring or diversity of failures, this is quite useful.

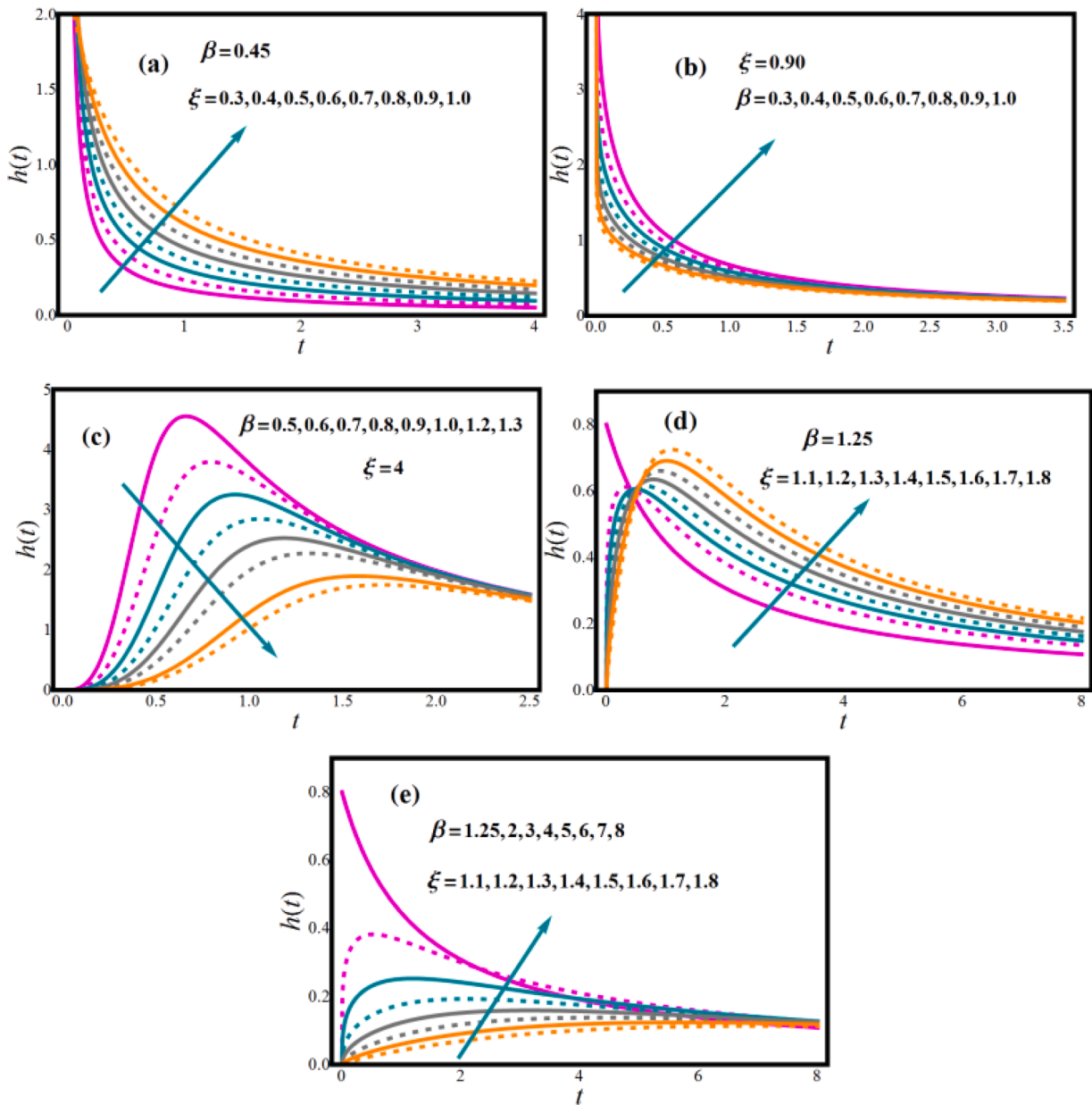


Fig. 4. Features of  $\xi$  and  $\beta$  on HRF

- It's easy to compare it to an exponential distribution.
- It is a specific form for the complete intensity single failure system.

The hazard rate function (HRF) of LL distribution

$$h(t|\xi, \beta) = \frac{\xi}{t} \left\{ 1 + \left(\frac{t}{\beta}\right)^{-\xi} \right\}^{-1}. \quad (5)$$

HRF function forms are depicted in Figs. 4 and 5. HRF is predicted in various forms, including declining, Uni-modal, and hump curve, all of which are desirable qualities for any lifetime model. Adaptable FRF forms with monotonic and non-monotonic hazard rate trends are common in real-time applications.

The cumulative hazard rate function (CHRF)  $C(t|\xi, \beta)$  is important in survival analyses. It determines the entire amount of risk incurred up to time  $t$ . The CHR of LL distribution

$$C(t|\xi, \beta) = \int_0^t h(y|\xi, \beta) dy = -\log[S(t|\xi, \beta)]. \quad (6)$$

Hence,

$$C(t|\xi, \beta) = \log \left\{ 1 + \left(\frac{t}{\beta}\right)^\xi \right\} \quad (7)$$

The parameters' impact on the CHRF profile is depicted in Fig. 6. The CHRF function of the LL distribution exhibits monotonously growing behavior.

The ratio between the PDF and its CDF is characterized as the reversed hazard rate (RHR) of a random life. This approach is helpful in interpreting censored data and can be employed in a wide range of discipline, such as forensic sciences. The RHR of  $T$  is determined as follows:  $h'(t|\xi, \beta) = f(t|\xi, \beta)[G(t|\xi, \beta)]^{-1}$  (see, explanations, characterizations, and other details, Ref. [23]). In the contemporary publications of dependability evaluation and stochastic modelling, the RHR has

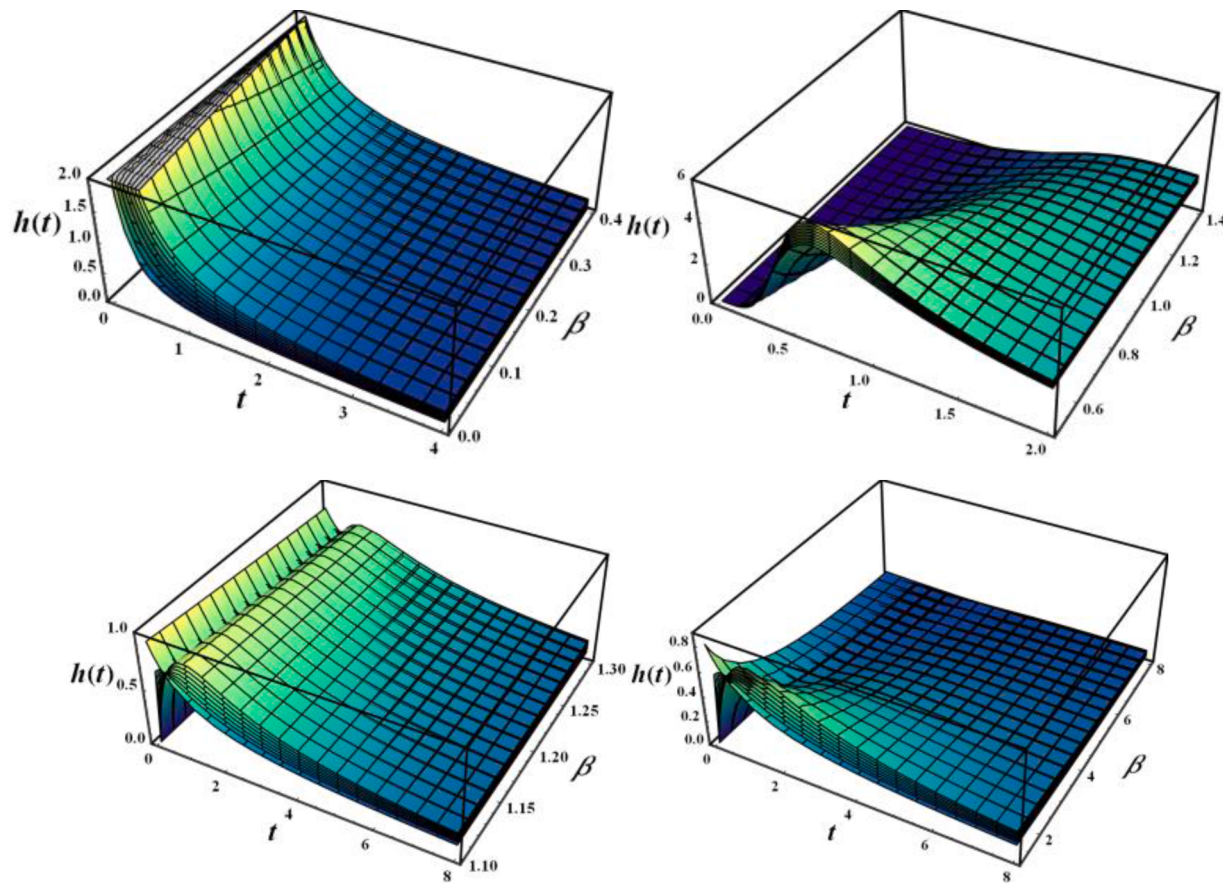


**Fig. 5.** 3D profile of HRF of LL distribution with rising  $\xi$ .

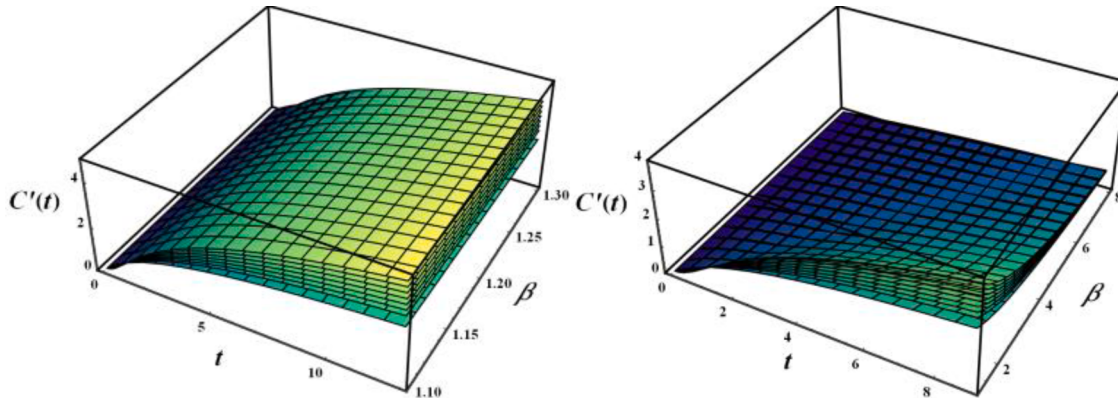


**Fig. 6.** Features of  $\xi$  and  $\beta$  on CHRF

received a lot of attention [24].

$$h'(t|\xi, \beta) = \frac{\xi}{t \left\{ 1 + \left( \frac{t}{\beta} \right)^{\xi} \right\}}. \quad (8)$$

**Fig. 7**

Because of its relationship to failure rate, Mills Ratio is a particular strategy for assessing durability.

$$MR(t|\xi, \beta) = \frac{S(t|\xi, \beta)}{f(t|\xi, \beta)} = \frac{t}{\xi} \left\{ 1 + \left( \frac{t}{\beta} \right)^{-\xi} \right\}. \quad (9)$$

**Fig. 8**

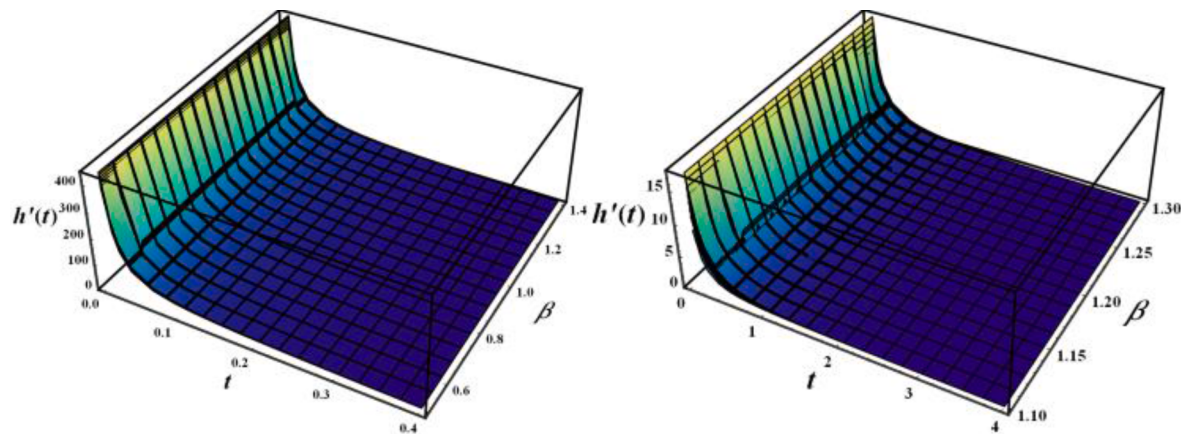
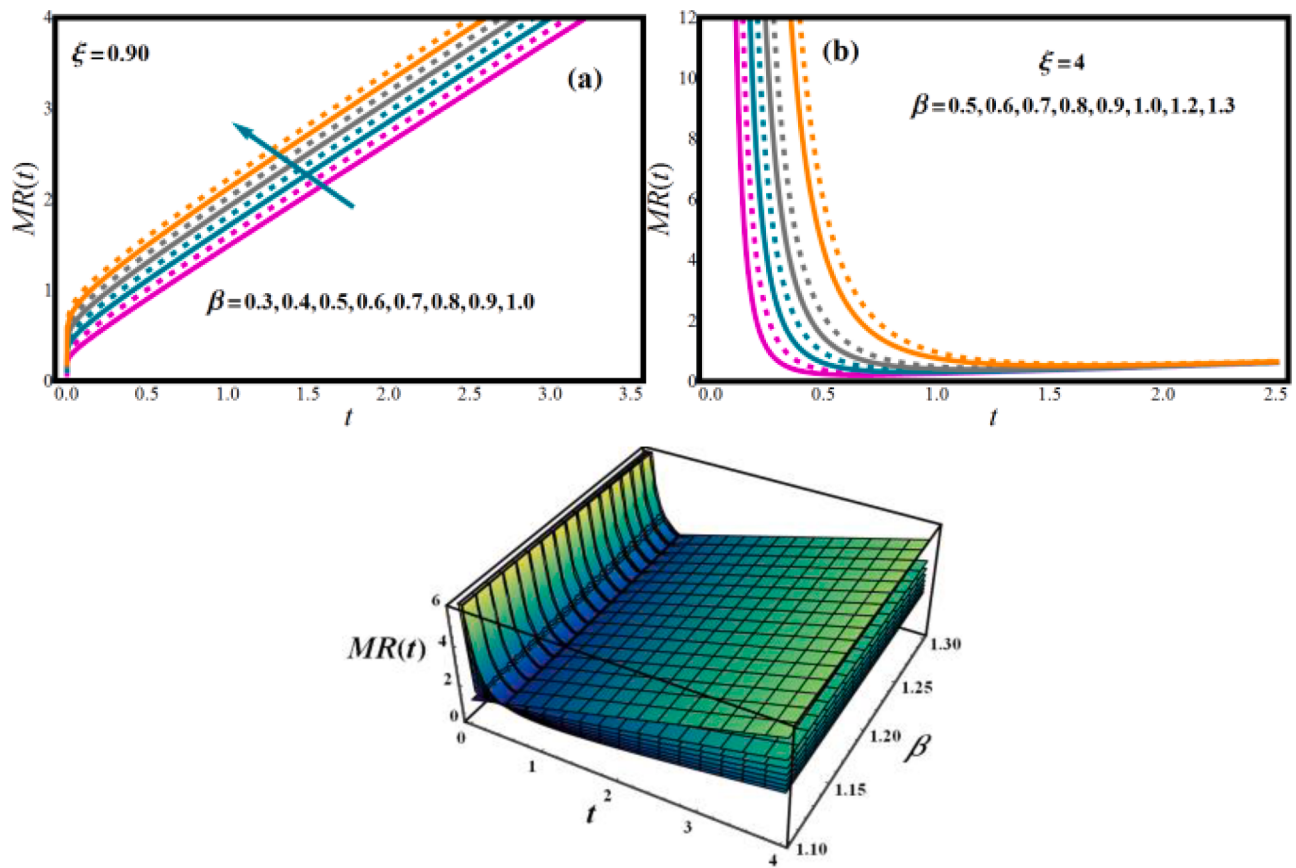
The odd function of  $T \bar{O}(t|\xi, \beta) = F(t|\xi, \beta)/S(t|\xi, \beta)$  is

$$OF(t|\xi, \beta) = \left\{ 1 + \left( \frac{t}{\beta} \right)^{-\xi} \right\}^{-1} \left\{ 1 + \left( \frac{t}{\beta} \right)^{\xi} \right\}. \quad (10)$$

**Fig. 9**

### 3. Solution methodology

Many parametric solution approaches have been proposed in the literature, but the MLE is the most extensively utilized. The maximum likelihood estimators  $\hat{\xi}, \hat{\beta}$  of  $\xi, \beta$  is a function of the given data that maximizes  $L(.)$  across all feasible scores of  $\xi, \beta$  in the parameter space as

Fig. 7. Features of  $\xi$  and  $\beta$  on RHRFFig. 8. Features of  $\xi$  and  $\beta$  on MR

a function of the given data. Let  $T_1, T_2, \dots, T_n$  are random sample and the related given values,  $t_1, t_2, \dots, t_n$  from LL distribution with parameters  $\xi, \beta$ .

The log-likelihood ( $\log L(\cdot)$ ) is usually less hard to maximize. Therefore  $l(\cdot)$  of  $T_1, T_2, \dots, T_n$  is

$$l(t|\xi, \beta) = \log \prod_{i=1}^n \left( \frac{\xi}{\beta} \right) \left( \frac{t_i}{\beta} \right)^{\xi-1} \left\{ 1 + \left( \frac{t_i}{\beta} \right)^\xi \right\}^{-2}, \quad (11)$$

$$\begin{aligned} l(t|\xi, \beta) &= n \log \xi - n \log \beta + (\xi - 1) \sum_{i=1}^n \log t_i - n(\xi - 1) \log \beta \\ &\quad - 2 \sum_{i=1}^n \log \left\{ 1 + \left( \frac{t_i}{\beta} \right)^\xi \right\}. \end{aligned} \quad (12)$$

We are now concentrating on obtaining the MLEs. To do so, we first maximize Eq. (12), then compute  $\frac{\partial l(\cdot)}{\partial(\cdot)}$  with respect to the unknown parameters and equate to zero. The score operator is the  $\log L(\cdot)$  derivative, and the score vector components  $U(\cdot)$  are provided by

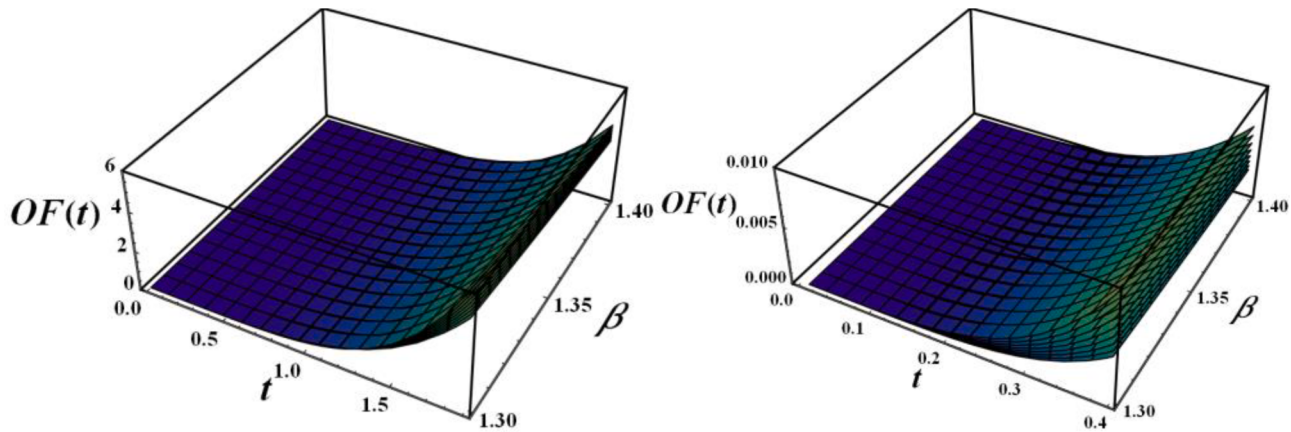
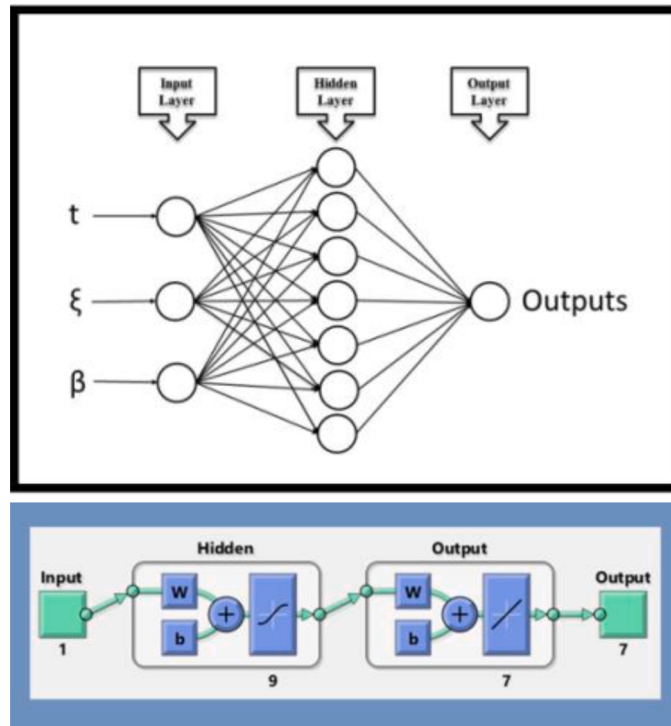
Fig. 9. Features of  $\xi$  and  $\beta$  on OF

Fig. 10. . (a) The symbolic architecture (top) (b) Basic configuration (bottom)

$$U(\xi, \beta) = \left[ \frac{\partial l(t|\xi, \beta)}{\partial \xi}, \frac{\partial l(t|\xi, \beta)}{\partial \beta} \right]^T. \quad (13)$$

Then  $\frac{\partial l(\cdot)}{\partial (\cdot)}$  w.r.t.  $\xi$  and  $\beta$  are:

$$\frac{\partial l(t|\xi, \beta)}{\partial \xi} = \frac{n}{\xi} + \sum_{i=1}^n \log t_i - n \log \beta - 2 \sum_{i=1}^n \frac{\left(\frac{t_i}{\beta}\right)^{\xi} \log \left(\frac{t_i}{\beta}\right)}{\log \left\{ 1 + \left(\frac{t_i}{\beta}\right)^{\xi} \right\}}, \quad (14)$$

$$\frac{\partial l(t|\xi, \beta)}{\partial \beta} = \frac{n}{\beta} - \frac{n(\xi - 1)}{\beta} + 2 \xi \sum_{i=1}^n \frac{\left(\frac{t_i}{\beta}\right)^{\xi}}{1 + \left(\frac{t_i}{\beta}\right)^{\xi}}, \quad (15)$$

This result of estimation is used in evaluation of survival analysis of LL distribution and has been authenticated and compared with ANN prediction discussed in Section 4.

#### 4. Basic equations and foundation of the ANN model design

Seven distinct parameters were estimated using a multilayer perceptron (MLP) ANN model. In the MLP network model's input layer, that is one of the most extensively employed ANN models,  $t$ ,  $\xi$  and  $\beta$  values are defined and RF, HRF, PDF, RHRF, Mills, OF and CHR parameters are obtained in the output layer [25–27]. Since there is no mechanism for detecting neurons in MLP networks' deep layer, the performances of ANNs formed with various neuron counts were assessed and the hidden layer model with 9 neurons was explored [26,28,29]. The symbolic framework and fundamental configuration of the adapted ANN model are shown in Fig. 10. The 34 of data points are reserved for training, 8 for confirmation, and 8 for testing in ANN model, which utilizes a number of 50 data [30–32]. Levenberg-Marquardt training algorithm, that has a strong learning structure, was employed as the training algorithm [33–35]. The Tan-Sig and PFs (Purelin functions) used as transfer functions are [25,36]:

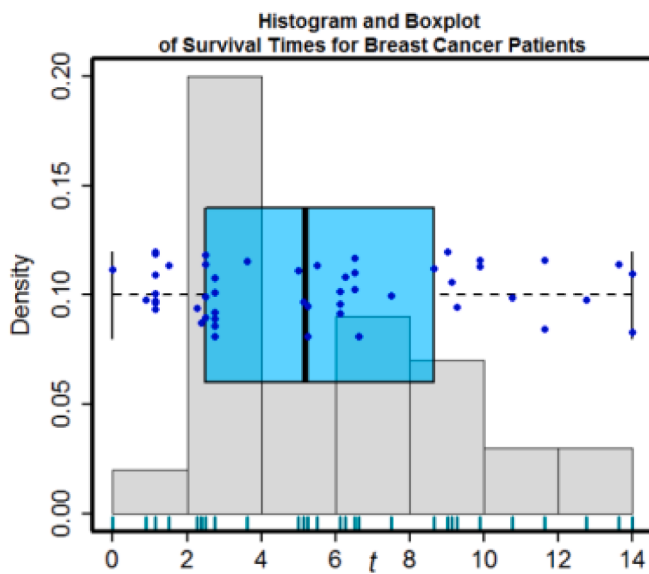


**Fig. 11.** Histogram and box plot for survival times of cancer patients' data.

$$f(x) = \frac{1}{1 + e^{-x}} \quad (16)$$

$$\text{purelin}(x) = x \quad (17)$$

In order to study the training and prediction behavior of ANN model, the behavior parameters, coefficient of determination ( $R$ ), margin of deviation (MoD) and mean squared error (MSE) scores that are frequently employed in research were chosen. The mathematical statements utilized in the calculation of the behavior parameters are [37–39]:

$$R = \sqrt{1 - \sum_{i=1}^N (X_{\text{targ}(i)} - X_{\text{pred}(i)})^2 \left\{ \sum_{i=1}^N (X_{\text{targ}(i)})^2 \right\}^{-1}} \quad (18)$$

$$\text{MOD} = 100 \times \left[ \frac{X_{\text{targ}} - X_{\text{pred}}}{X_{\text{targ}}} \right] \quad (19)$$

$$\text{MSE} = N^{-1} \sum_{i=1}^N (X_{\text{targ}(i)} - X_{\text{pred}(i)})^2 \quad (20)$$

## 5. Numerical approach and ANN validation

In this section, we look at how LL distribution has been implemented on data obtained from 50 breast cancer patients at Medical City Hospital in Baghdad in the year 2020. As of the time of the patient's admission to the hospital till discharge, and as of the time of their release, all of them were dead; this data is regarded complete data. The distribution of data is LL. The more detail about the data can be seen in [40]. They had used Anderson-Darling, Chi-squared, and Kolmogorov-Smirnov statistic as model fitting requirement; and the LL model fits all of the requirements for a greater goodness fit model, according to the findings of this study.

The following are the findings of their investigation into the MLEs of parameters for this data:  $\hat{\beta} = 3.2795$  and  $\hat{\xi} = 4.8896$ . Histograms and box plots are both employed to investigate and display data in a simple and concise way. Since histograms are more effective in displaying data distribution, a box plot can be helpful to determine whether the distribution is symmetric or skewed. Fig. 11 exhibits histogram and boxplot plots, demonstrating that the distribution is right-skewed. Using these results, we were able to analyze the effects of MLEs of key parameters on the FF, RF, HRF, RHRF, MR, OF and CHRF for cancer patients' survival periods and forecast these outcomes applying an ANN framework. The accuracy of the outcome was determined by calculating these scores for

the survival measures of interests for the  $\hat{\beta} = 3.2795$  and  $\hat{\xi} = 4.8896$ .

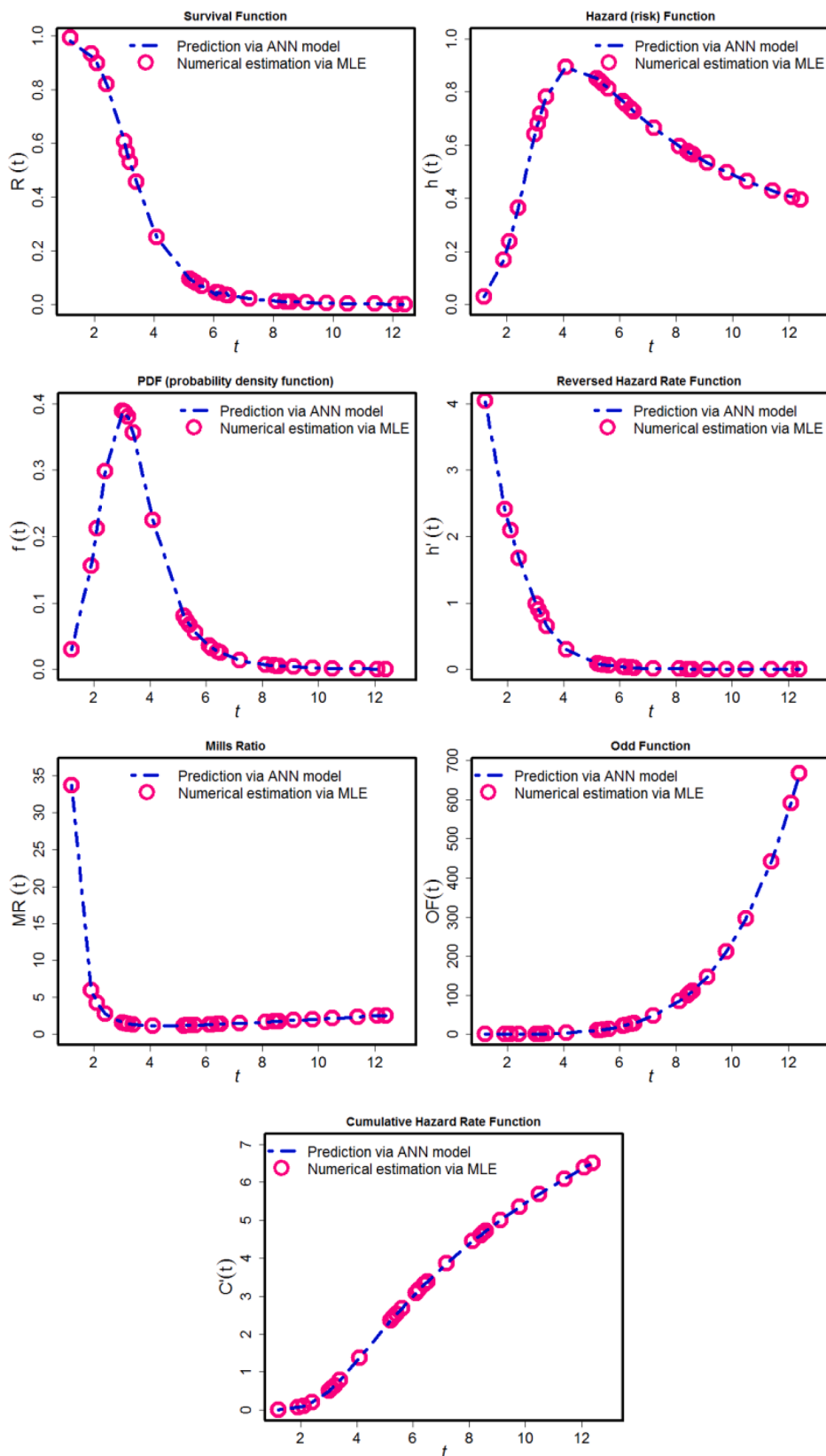
Fig. 12 depicts the behavior of survival function indicators for cancer patients' survival periods using the MLE technique and ANN prediction. The both results have been authenticated and compared through graphically. It is seen that graphs are almost identical under both methods. We notice from Fig. 12, that the survival function, Mills ratio and RHRF appeared decreasing, and the risk function appeared upside down bathtub shaped, and this corresponds to the theory of the functions. Whereas, In this line, an increment of survival time causes the boost in the profile of odd function and CHRF, as indicated in Fig. 12. This corresponds to the theory of the functions discussed in Section 3. These have been demonstrated to be in excellent accordance when compared to the ANN model and we obtained an excellent confirmation of the results as shown in Fig. 12. As a conclusion, the current study can be used to analyze survival study issues with confidence.

## 6. Results and discussion

Before examining the accuracy of the prediction of the ANN model, it is pivotal to verify that the training phase is preferably finished. Fig. 13 provides the training performance of the MLP network. Although MSE estimates are large in the early phases of the MLP network, MSE values drop with each successive epoch. The decrease in MSE values shows that the error between the predicted scores and the target outcomes obtained in output layer also decreases. By the 15<sup>th</sup> epoch, the smallest error value was acquired and the training stage of model was terminated by achieving the highest training performance. This indicates that the training phase of the MLP architecture was finished with a very low error rate. Fig. 14 predicts error histogram of ANN model. In the error histograms, the training performance of the model is analyzed by showing the differences across the predicted scores and the target scores. When the results in the error histogram are scrutinized, it is noticed that the values obtained of the errors are really near to zero and are extremely low. It's also worth mentioning that the errors are concentrated near the zero error line. The results obtained from the error histogram show that the errors for the training phase of the ANN model are very low and the training phase of the model is completed ideally. The ANN model's  $R$  score was found to be 0.99958. And this is another indication of the ideal completion of the training phase of the model. In Fig. 15, for each of the 7 output values, the agreement of the target values with the predicted values is examined. When the values shown for each of the 50 data used in the development of the ANN model are examined, it is seen that the predicted values obtained from the ANN model are in perfect agreement with the target values. Fig. 16 shows the MoD values calculated for each data point. When the values calculated to analyze the prediction errors of the ANN model are analyzed, it is seen that the MoD values for 50 data points are generally on or very close to the zero deviation line. It should be noted that the average MoD quantities provided for each output are also quite low. Results gleaned from the calculated MoD quantities show that ANN model can calculate 7 output values with very low deviation values. Another error analysis was made in Fig. 17, where the disparities in target values and ANN outputs were scrutinized. The low difference values are considered as another proof that the ANN model can make forecasts with very small errors. In Fig. 18, on the x and y axes, the target and output values are displayed, respectively. It's worth noting that the positions of the data points are on the zero error line and are in  $\pm 10\%$  error band. The study found that the designed ANN model is capable of accurately predicting each output value with very minimal errors.

## 7. Conclusions

In this research work, comparative examination of the MLE method and ANN modeling has been scrutinized using LL distribution. This innovative model has been applied in a survival-based examination of

**Fig. 12.** Validity of results.

cancer patients' remission periods and survival times. In recent decades, several attempts have been undertaken to combat cancer by combining modern technologies with traditional methods. As general non-linear models, artificial neural networks have been demonstrated to be

effective in medical diagnosis, forecasting, and survival analysis.

The important findings are noted as follows:

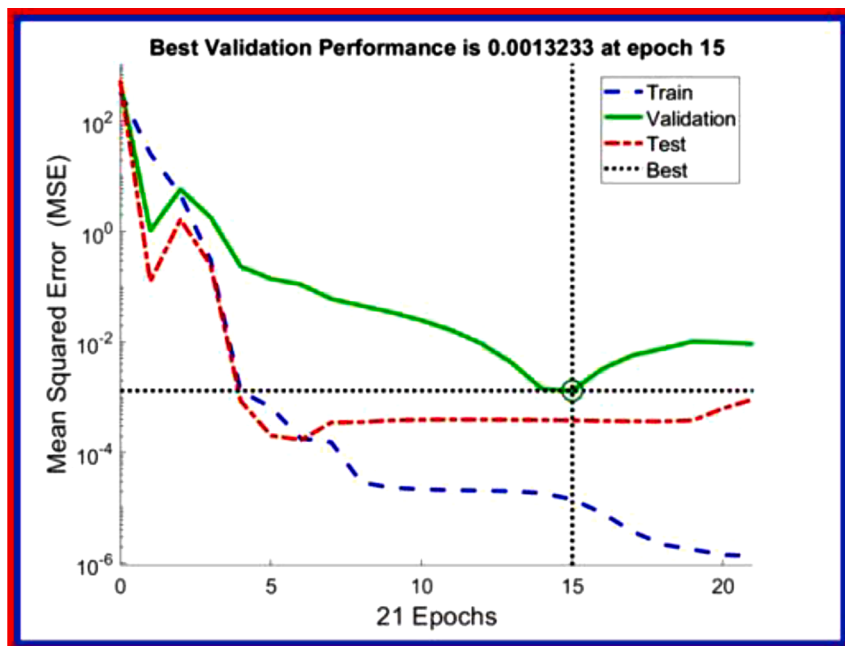


Fig. 13. The MLP network's training efficiency

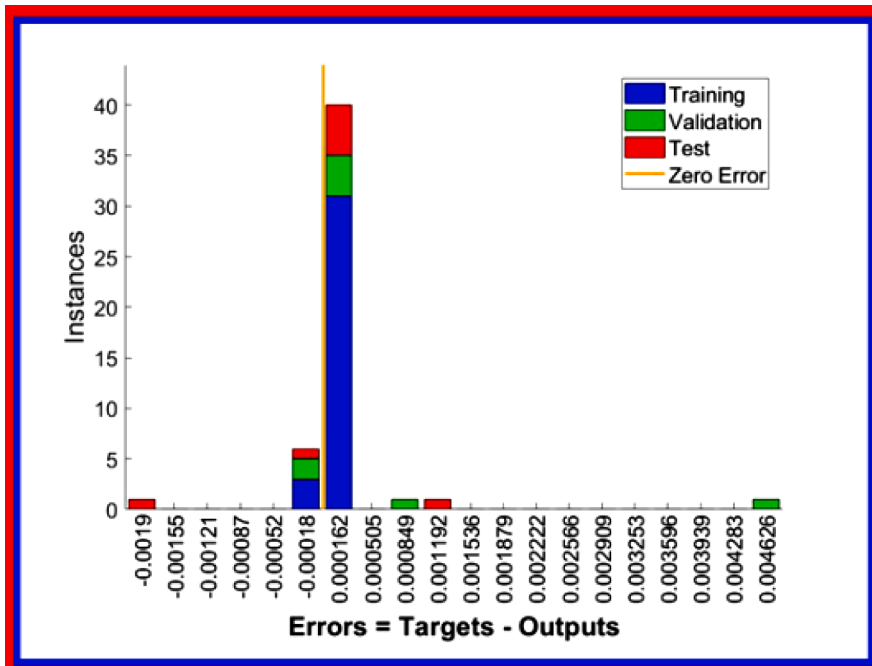
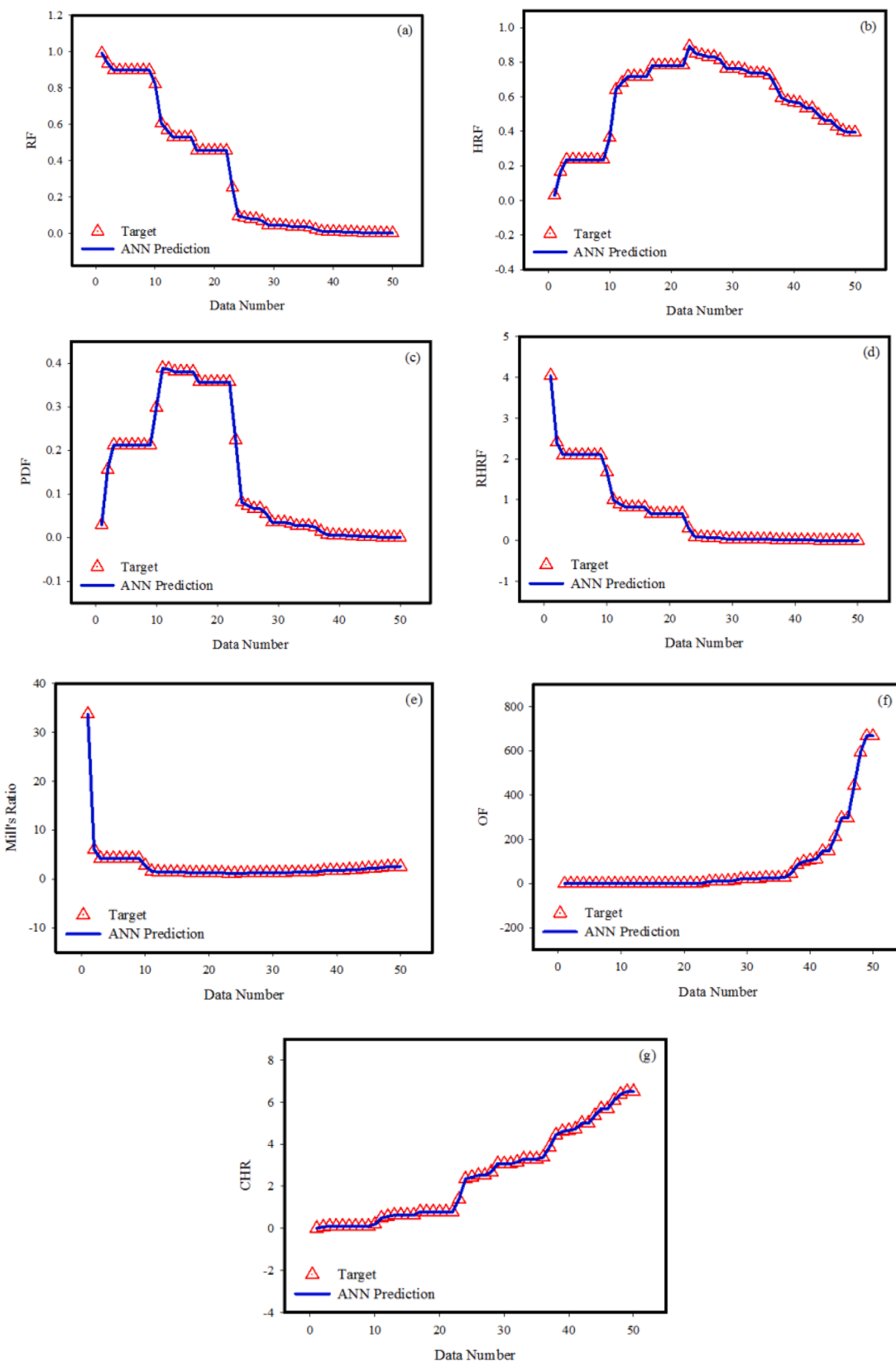


Fig. 14. An ANN model's error histogram

- Through the results of the ANN experiments, survival characteristics of LL distribution like survival/reliability, risk, and others functions can be predicted more precisely.
- It has been revealed that both strategies exhibit the same pattern as the time increases.
- The values of the risk function increase with the increase in the time of infection and then decrease for a group of breast cancer patients under study, which corresponds to the theoretical properties of this function as it is an upside down bathtub shaped function, according to the practical conclusions.
- The values of the survival function appeared decreasing as the values of  $(t)$  increased, and this corresponds to the theory of the SF.

- As survival time ' $t$ ' rose, the values of the survival function seemed to be diminishing, this is consistent with the survival function theory.
- The probability density function's results gradually increased before declining.
- The R value for the developed ANN model was calculated as 0.99958.
- The MoD value assessed for each of the 7 out-turns parameters estimated by the ANN model was very low.
- The findings of the investigation of performance parameters revealed that ANNs are an excellent technique that can be used in the analysis of survival of cancer patients.

It is important to note that the findings obtained by utilizing ANN



**Fig. 15.** The outputs received from the ANN model and the target values

experiments and maximum likelihood method are close enough in the current study. Other researchers may be able to draw inspiration from the current study to conduct future research further into the ANN modelling of the lifetime distribution with different scenarios.

#### Data availability statement

The datasets generated and analyzed during the current research are available from the corresponding author on reasonable request.

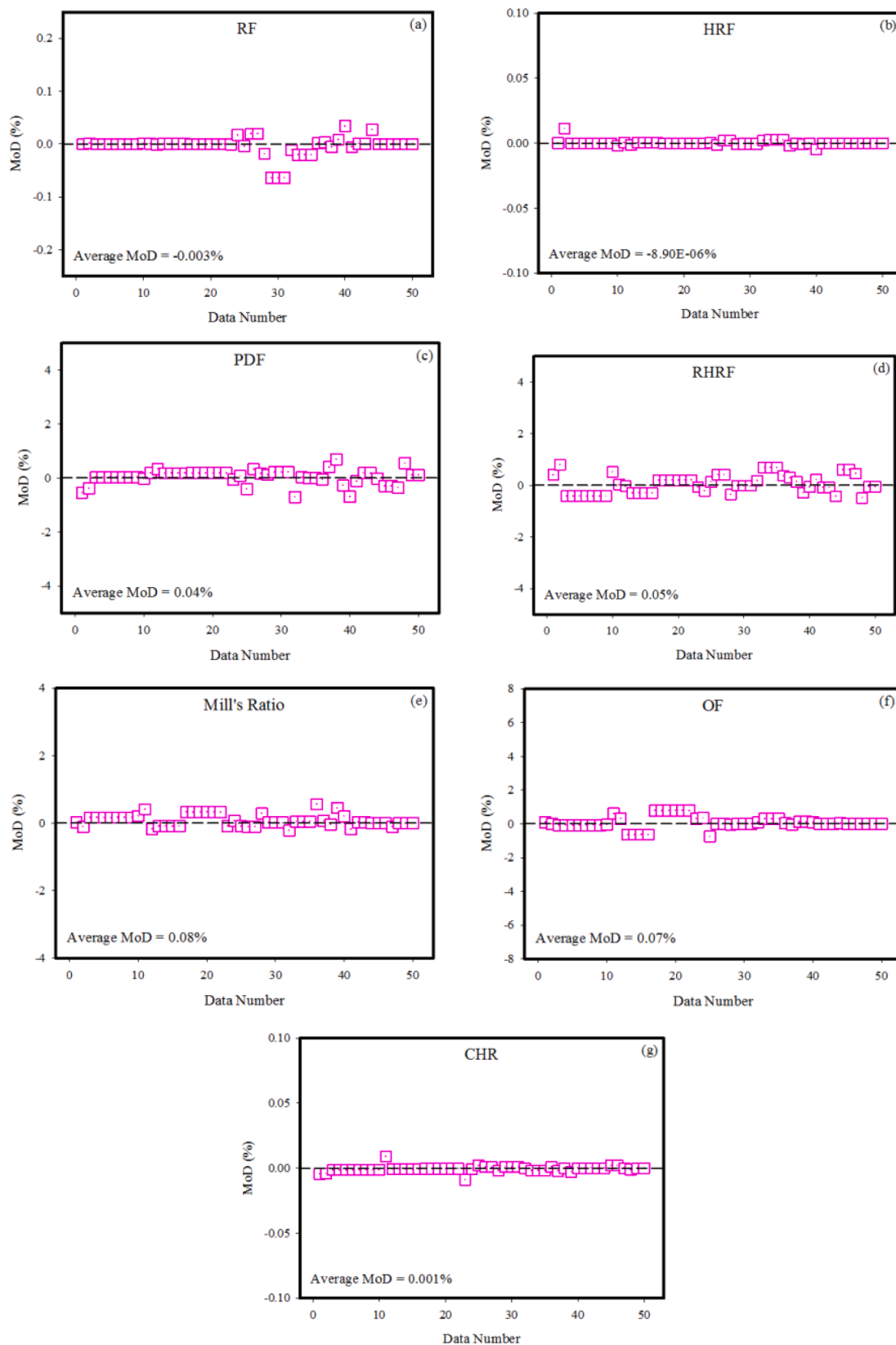
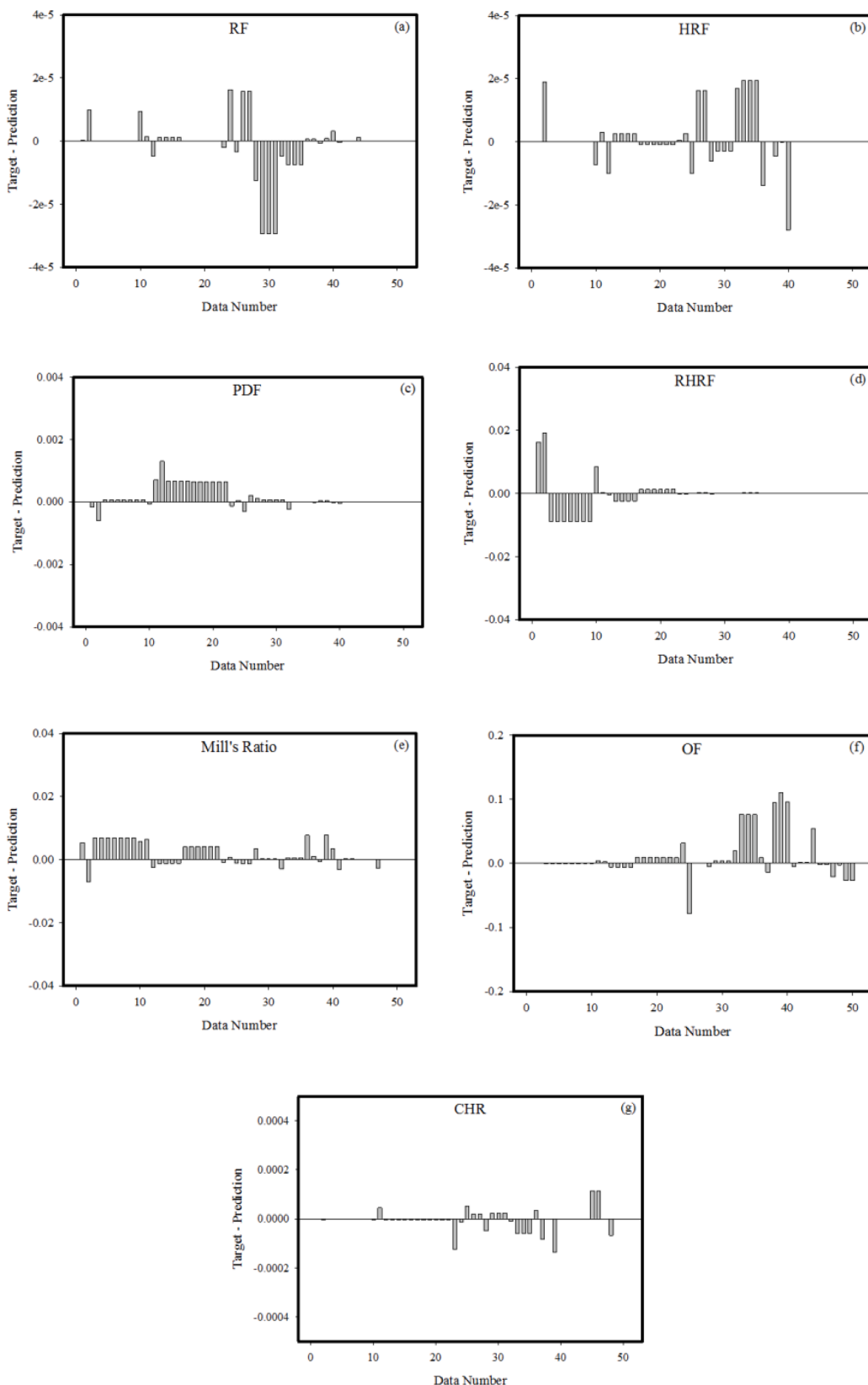


Fig. 16. The target data and the outputs received from the ANN model

#### CRediT authorship contribution statement

**Anum Shafiq:** Conceptualization, Investigation, Methodology, Software, Supervision, Writing – original draft, Writing – review &

editing. **Andaç Batur Çolak:** Conceptualization, Investigation, Software, Validation, Writing – original draft, Writing – review & editing. **Tabassum Naz Sindhu:** Conceptualization, Formal analysis, Investigation, Methodology, Validation, Writing – original draft, Writing – review



**Fig. 17.** The disparities between the target data and the outputs of the ANN

& editing. **Showkat Ahmad Lone:** Conceptualization, Methodology, Writing – original draft. **Tahani A. Abushal:** Conceptualization, Formal analysis, Methodology, Resources, Software.

#### Declaration of Competing Interest

The authors declare that they have no known competing financial interests or personal relationships that could have appeared to influence

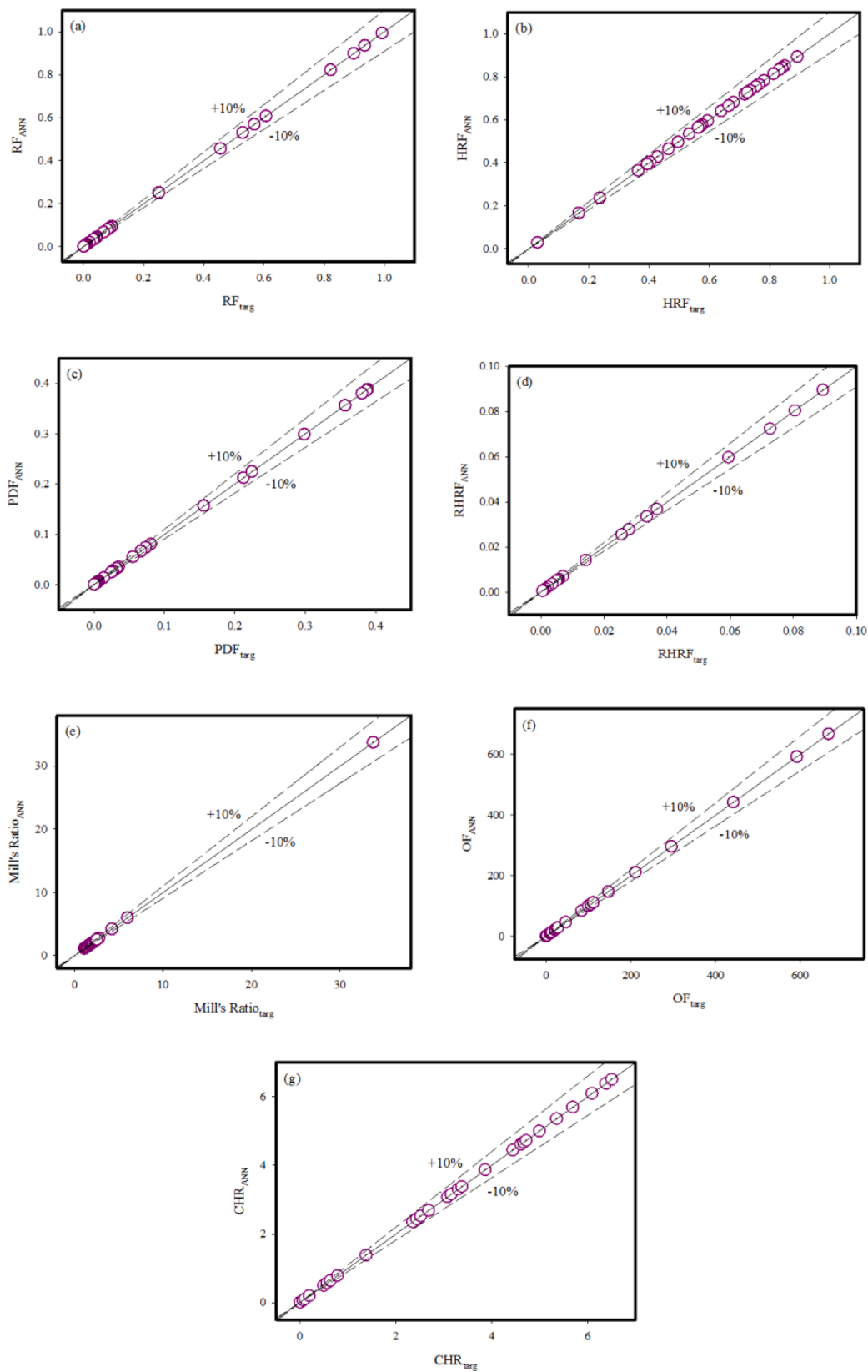


**Fig. 18.** The discrepancy ratios between the target data and the forecast values derived from the ANN model

the work reported in this paper.

## Data availability

No data was used for the research described in the article.

## Acknowledgment

The authors would like to thank the Deanship of Scientific Research at Umm Al-Qura University for supporting this work by Grant Code 22UQU4310063DSR14.

## References

- [1] Achieve Clinical Research. (2012). The anxiety over breast cancer recurrence. Retrieved from <http://www.achieveclinical.com/news/the-anxiety-over-breast-cancer-recurrence/>.
- [2] American Cancer Society. (2010). Cancer facts & figures. Retrieved from <http://www.cancer.org/Research/CancerFactsFigures/>.
- [3] American Cancer Society. (2012). Learn about cancer: breast cancer. Retrieved from <http://www.cancer.org/cancer/breastcancer/detailedguide/breast-cancer-key-statistics>.
- [4] Perou CM, et al. Molecular portraits of human breast tumours. *Nature* 2000;406(6797):747–52.
- [5] Garcia-Closas, et al. Heterogeneity of breast cancer associations with five susceptibility loci by clinical and pathological characteristics. *PLoS Genet* 2008;4(4):e1000054.
- [6] Colditz GA, Rosner BA, Chen WY, Holmes MD, Hankinson SE. Risk factors for breast cancer according to estrogen and progesterone receptor status. *J Natl Cancer Inst* 2004;96(3):218–28.
- [7] Berg WA, et al. Detection of breast cancer with addition of annual screening ultrasound or a single screening MRI to mammography in women with elevated breast cancer risk. *JAMA* 2012;307(13):1394–404.
- [8] Kourou K, Exarchos TP, Exarchos KP, Karamouzis MV, Fotiadis DI. Machine learning applications in cancer prognosis and prediction. *Comput Struct Biotechnol J* 2015;13:8–17.
- [9] Huang C, Clayton EA, Matyunina LV, McDonald L, Benigno BB, Vannberg F, McDonald JF. Machine learning predicts individual cancer patient responses to therapeutic drugs with high accuracy. *Sci Rep* 2018;8(1):1–8.
- [10] Bibault JE, Giraud P, Burgun A. Big data and machine learning in radiation oncology: state of the art and future prospects. *Cancer Lett* 2016;382(1):110–7.
- [11] Ambrogi F, Lama N, Boracchi P, Biganzoli E. Selection of artificial neural network models for survival analysis with genetic algorithms. *Comput Stat Data Anal* 2007;52(1):30–42.
- [12] Shafiq A, Çolak AB, Sindhu TN, Lone SA, Alsabie A, Jarad F. Comparative study of artificial neural network versus parametric method in COVID-19 data analysis. *Results Phys* 2022;105613.
- [13] Bhambhvani HP, et al. Development of robust artificial neural networks for prediction of 5-year survival in bladder cancer. *Urologic oncology: seminars and original investigations*, 39. Elsevier; 2021. 3193-e7.
- [14] Ragab A, Green J. On order statistics from the log-logistic distribution and their properties. *Commun Theory Methods* 1984;13(21):2713–24.
- [15] Ashkar F, Mahdi S. Fitting the log-logistic distribution by generalized moments. *J Hydrol* 2006;328(3-4):694–703.
- [16] Bennett S. Log-logistic regression models for survival data. *Journal of the Royal Statistical Society: Series C (Applied Statistics)* 1983;32(2):165–71.
- [17] Collett D. Modelling survival data in medical research. CRC Press; 2015.
- [18] Shoukri MM, Mian IUH, Tracy DS. Sampling properties of estimators of the log-logistic distribution with application to Canadian precipitation data. *Can J Stat* 1988;16(3):223–36.
- [19] Ali MM, Khan AH. On order statistics from the log-logistic distribution. *J Stat Plan Inference* 1987;17:103–8.
- [20] Miller RG. Survival analysis. New York: Wiley; 1981.
- [21] Cox DR, Oakes DD. Analysis of survival data. New York: Chapman and Hall; 1984.
- [22] Cox C, Chu H, Schneider MF, Munoz A. Parametric survival analysis and taxonomy of hazard functions for the generalized gamma distribution. *Stat Med* 2007;26(23):4352–74.
- [23] Block HW, Savits TH, Singh H. The reversed hazard rate function. *Probab Eng Inf Sci* 1998;12(1):69–90.
- [24] Gupta RD, Nanda AK. Some results on reversed hazard rate ordering. *Commun Theory Methods* 2001;30(11):2447–57.
- [25] Wang J, Ayari MA, Khandakar A, Chowdhury ME, Uz Zaman SA, Rahman T, Vaferi B. Estimating the relative crystallinity of biodegradable polylactic acid and polyglycolide polymer composites by machine learning methodologies. *Polymers* 2022;14(3):527.
- [26] Shafiq A, Çolak AB, Naz Sindhu T. Designing artificial neural network of nanoparticle diameter and solid–fluid interfacial layer on single-walled carbon nanotubes/ethylene glycol nanofluid flow on thin slendering needles. *Int J Numer Methods Fluids* 2021;93(12):3384–404.
- [27] Shafiq A, Çolak AB, Swarup C, Sindhu TN, Lone SA. Reliability analysis based on mixture of lindley distributions with artificial neural network. *Adv Theory Simul* 2022;5(8):2200100. <https://doi.org/10.1002/adts.202200100>.
- [28] Bonakdari H, Zaji AH. Open channel junction velocity prediction by using a hybrid self-neuron adjustable artificial neural network. *Flow Meas Instrum* 2016;49:46–51.
- [29] Shafiq A, Çolak AB, Lone SA, Sindhu TN, Muhammad T. Reliability modeling and analysis of mixture of exponential distributions using artificial neural network. *Math Methods Appl Sci* 2022. <https://doi.org/10.1002/mma.8178>.
- [30] Esmaeilzadeh F, Teja AS, Bakhtyari A. The thermal conductivity, viscosity, and cloud points of bentonite nanofluids with n-pentadecane as the base fluid. *J Mol Liq* 2020;300:112307.
- [31] Barati-Harooni A, Najafi-Marghamaleki A. An accurate RBF-NN model for estimation of viscosity of nanofluids. *J Mol Liq* 2016;224:580–8.
- [32] Rostamian SH, Biglari M, Saedodin S, Esfe MH. An inspection of thermal conductivity of CuO-SWCNTs hybrid nanofluid versus temperature and concentration using experimental data, ANN modeling and new correlation. *J Mol Liq* 2017;231:364–9.
- [33] Ali A, Abdulrahman A, Garg S, Maqsood K, Murshid G. Application of artificial neural networks (ANN) for vapor-liquid-solid equilibrium prediction for CH4-CO2 binary mixture. *Greenh Gases: Sci Technol* 2019;9(1):67–78.
- [34] Abdul Kareem FA, Shariff AM, Ullah S, Garg S, Dreisbach F, Keong LK, Mellon N. Experimental and neural network modeling of partial uptake for a carbon dioxide/methane/water ternary mixture on 13X zeolite. *Energy Technol* 2017;5(8):1373–91.
- [35] Çolak AB, Karakoyun Y, Acikgoz O, Yumurtaci Z, Dalkilic AS. A numerical study aimed at finding optimal artificial neural network model covering experimentally obtained heat transfer characteristics of hydronic underfloor radiant heating systems running various nanofluids. *Heat Transf Res* 2022;53(5).
- [36] Akhgar A, Toghraie D, Sina N, Afrand M. Developing dissimilar artificial neural networks (ANNs) to prediction the thermal conductivity of MWCNT-TiO2/Water-ethylene glycol hybrid nanofluid. *Powder Technol* 2019;355:602–10.
- [37] Çolak AB, Sindhu TN, Lone SA, Akhtar MT, Shafiq A. A comparative analysis of maximum likelihood estimation and artificial neural network modeling to assess electrical component reliability. *Qual Reliab Eng Int* 2023.
- [38] Çolak AB, Shafiq A, Sindhu TN. Modeling of Darcy–Forchheimer bioconvective powell eyring nanofluid with artificial neural network. *Chin J Phys* 2022;77:2435–53.
- [39] Cao Y, Kamrani E, Mirzaei S, Khandakar A, Vaferi B. Electrical efficiency of the photovoltaic/thermal collectors cooled by nanofluids: machine learning simulation and optimization by evolutionary algorithm. *Energy Rep* 2022;8:24–36.
- [40] Hassan SS, Doori FA, Arebe E. Estimating the survival and risk functions of a log-logistic distribution by using order statistics with practical application. *Int J Nonlinear Anal Appl* 2022;13(1):2483–502.